Advanced Surfaces:
Their Tailoring and Analysis

Nicholas D. Spencer*

Abstract. Advanced surfaces constitute an important component in numerous high technologies today, both industrial and medical. In the Laboratory for Surface Science and Technology at the ETH-Zürich, many different surface treatments and processes are being examined, and novel techniques for the examination of such surfaces are also being developed. Among the modification methods described in this review are self-assembled monolayers, chemical vapor deposition, and surface functionalization with peptides. Novel analytical approaches include the extension of atomic force microscopy to allow surface-chemical analysis of oxides and polymers with high spatial resolution, and a waveguide technique, adapted to enable the *in situ* monitoring of protein adsorption on oxides of relevance to implant applications.

1. Introduction

The Laboratory for Surface Science and Technology in the Department of Materials, ETH-Zürich, was founded in 1993. The guiding principle of the group is that the ideal material for many applications consists of a combination of appropriate bulk properties (*e.g.*, *Young*'s modulus, electrical conductivity, cost) with appropriate surface properties (*e.g.*, specific binding of biomolecules, wear resistance).

The challenge is to create such materials by surface modification of bulk materials and to determine, by means of suitable surface-analytical techniques, whether the desired structures and chemistries of the bulk-surface system have been achieved. A different but closely related activity is the surface analysis of materials systems, whose performance is well-known, but whose surface composition and/or structure are not properly understood. This information may, of course, be fed back into the design of new surface-bulk combinations.

The principal application areas that have concerned us in the past five years have been biomaterials and tribology. Both represent technologies where the desired properties are quite well-understood on an empirical basis, but where little is known about the critical surface mechanisms that determine these properties. Some of the reasons for this knowledge gap are cultural. Biologists and those involved in clinical medicine are rarely familiar with surface analysis techniques, and the surface scientist only has received biological or medical training in exceptional cases. In tribology, the most significant split is between the mechanical engineer and the physicist or chemist, who are generally unfamiliar with each other's literature and methods. These problems require educational solutions. However, some of the reasons for the gap are technical: the systems are often complex and nonuniform, they do not lend themselves to analysis under the ultrahigh-vacuum conditions often employed in surface analysis, or analysis is necessary *in situ*, while the

Correspondence: Prof. Dr. N.D. Spencer
Laboratory for Surface Science and Technology
Department of Materials
ETH-Zürich NO H64
CH–8092 Zürich
Tel.: +41 1 632 58 50
Fax: +41 1 633 10 27
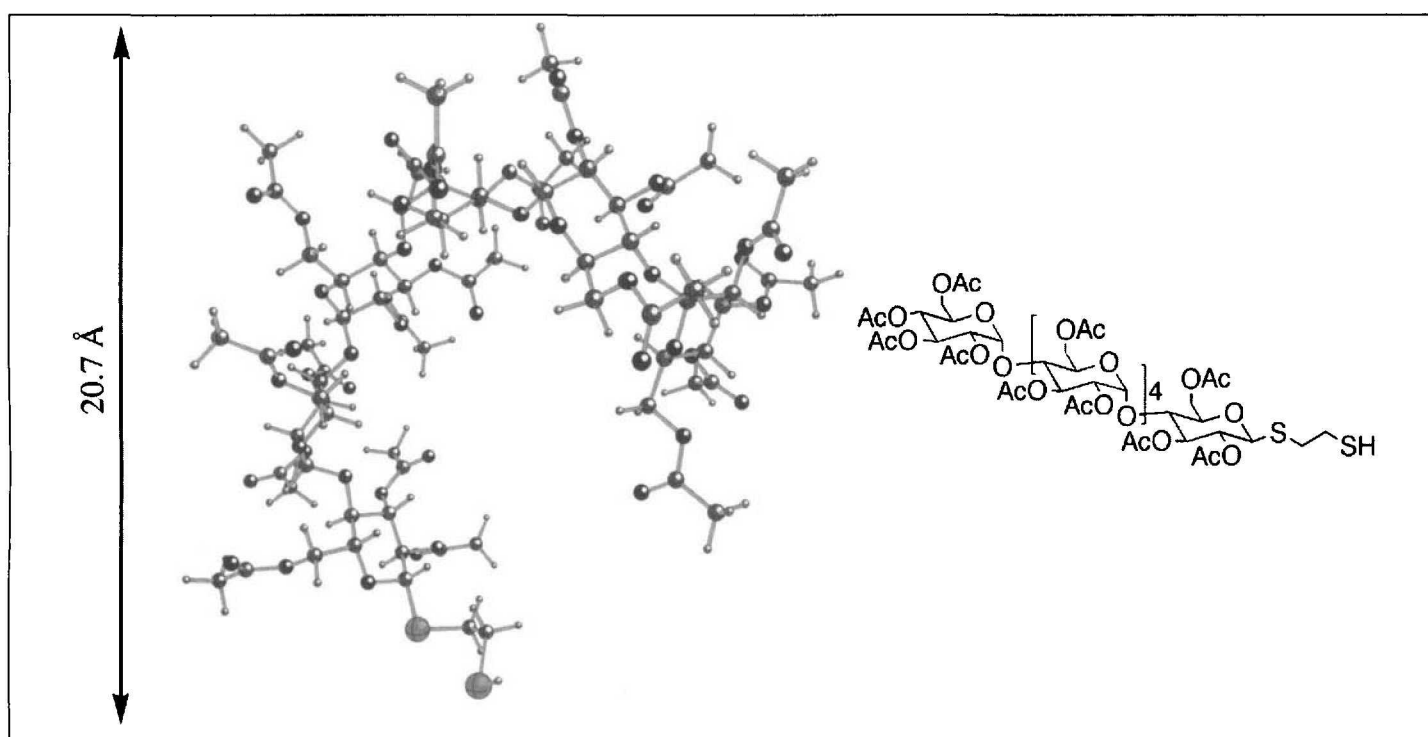E-Mail: nspencer@surface.mat.ethz.ch

Fig. 1. *2-Mercaptoethyl O-(2,3,4,6-tetra-O-acetyl-α-D-glucopyranosyl)-(1→4)-tetrakis[O-(2,3,6-tri-O-acetyl-α-D-glucopyranosyl)-(1→4)]-2,3,6-tri-O-acetyl-1-thio-β-D-glucopyranoside – corresponds to a thiol-terminated version of the first six units of amylose* (acetyl-protected) [2]

material is in a biological or tribological environment. These problems need to be addressed by the application, and often the development, of new analytical techniques.

2. Tailored Surfaces with Potential Biomedical Applications

Among the most versatile, effective, and simple technologies developed over the last few years for surface modification has been the self-assembled monolayer (SAM) [1]. The technique in its most frequently investigated incarnation involves the reaction of SH-terminated alkanes (containing a chain of at least twelve C-atoms) with a gold (111) surface (readily prepared by thermal deposition of gold on a flat surface such as mica) to form a monolayer. Thanks to the *van der Waals* interactions between the molecules, functionalities incorporated in the ω-position of the molecule are then exposed in an often highly ordered layer of concentrated functionality. We have used this thiol-gold chemistry in several applications of potential biomedical interest, including the anchoring of dense layers of oligosaccharides [2] *(Fig. 1)* and succinamide-containing species [3] *(Fig. 2)* on a surface. The oligosaccharides, which have been implicated in a number of molecular recognition mechanisms, could be adsorbed in different surface densities depending on whether the OAc protecting

groups are removed before or after adsorption of the monolayer. This presents the possibility of using different protecting group sizes as a way of controlling the distance between adsorbed oligosaccharides and thus probing receptor spacing in subsequent cell-adhesion studies. The succinamide layers have the useful property of being able to react with and thus immobilize NH_2-containing species, including peptides, proteins, and even viruses on a

surface. In this work, we also used the recently developed technique of micro-contact printing [4], in order to 'stamp' a pattern of the thiol onto the surface using a printing block made of polydimethylsiloxane, which had been patterned by pouring the monomer onto a lithographically produced test pattern prior to curing and was subsequent 'inked' with the thiol. Examples of collagen and Semliki Forest viruses that have been patterned in this
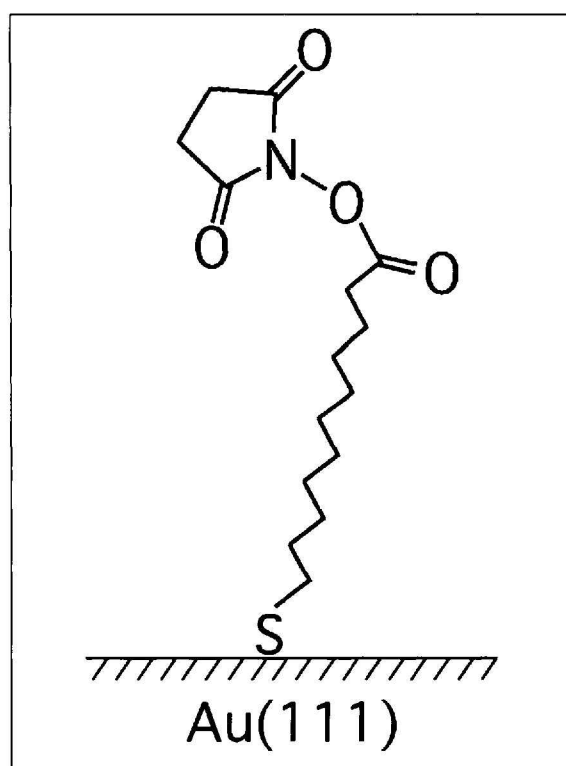

Fig. 2. *11,11'-Dithiobis(succinimidyl undecanoate)(DSU) dissociatively adsorbed on a gold surface* [3]
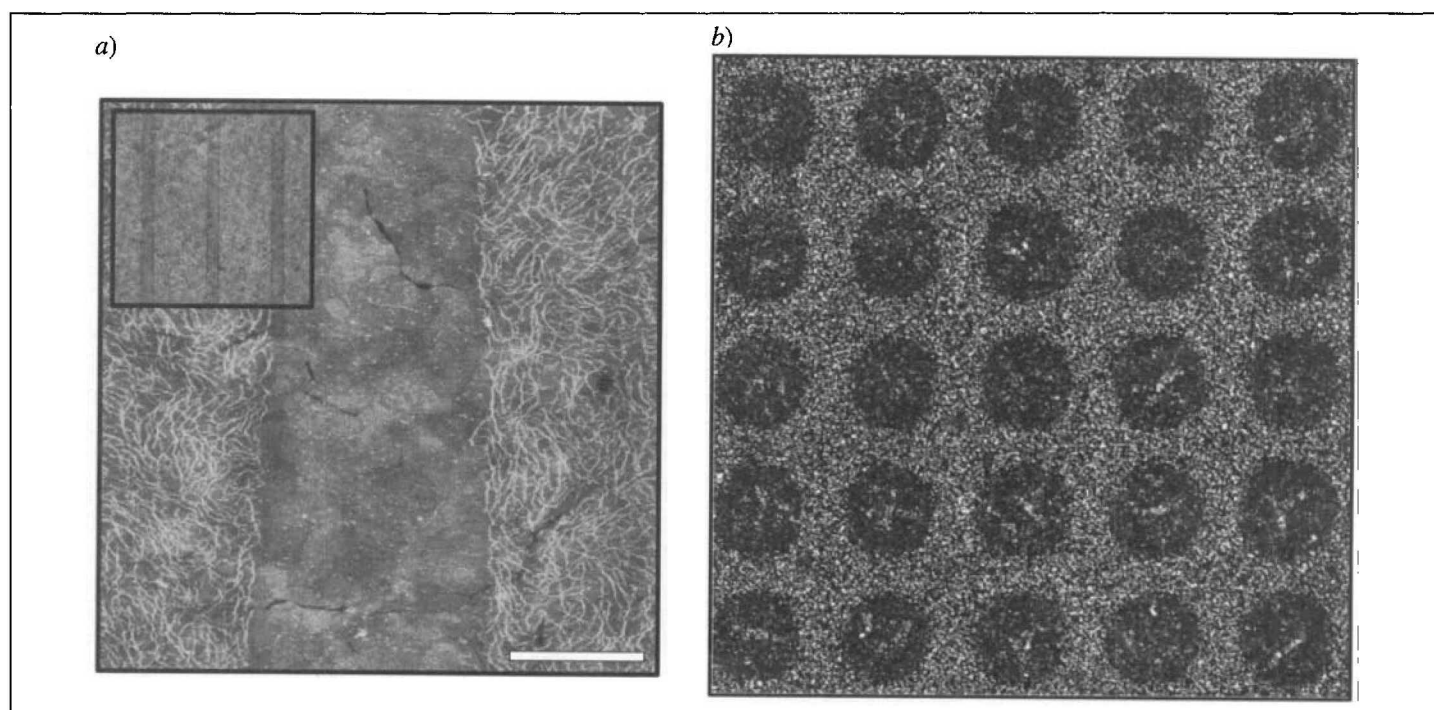

Fig. 3. *a) AFM image of a patterned network of collagen V molecules covalently immobilized on a DSU monolayer.* Bar = 1 μm. Inset: the same surface at 18 × lower mag. *b) AFM image of Semliki Forest viruses* (AFM-measured height 30 nm) *immobilized on a patterned DSU monolayer on a gold surface.* The diameter of the circular areas is 4.5 μm [3].

APTES: 3-aminopropyltriethoxysilane
EMCS: N-succinimidyl-6-maleimidylhexanoate
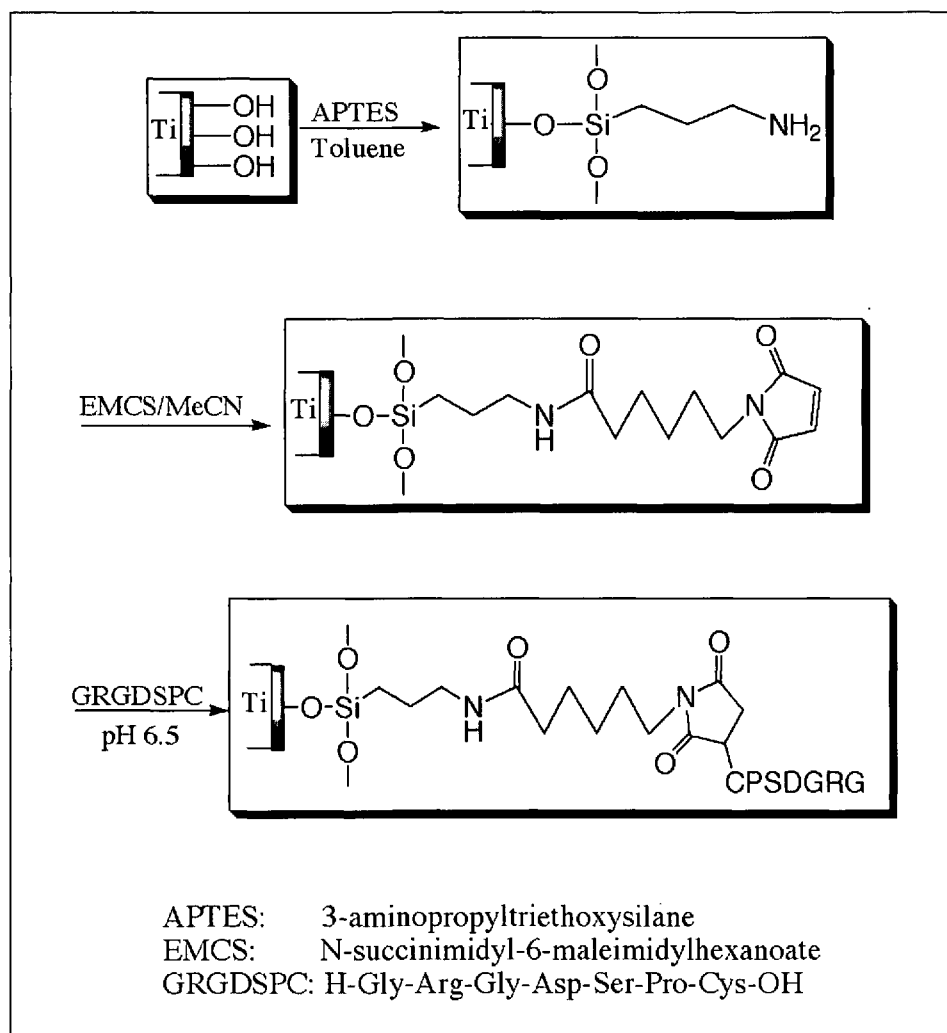GRGDSPC: H-Gly-Arg-Gly-Asp-Ser-Pro-Cys-OH

Fig. 4. *Chemical reaction sequence chosen to covalently immobilize specific, cell-adhesive peptides on the surface of titanium (oxide)* [8]
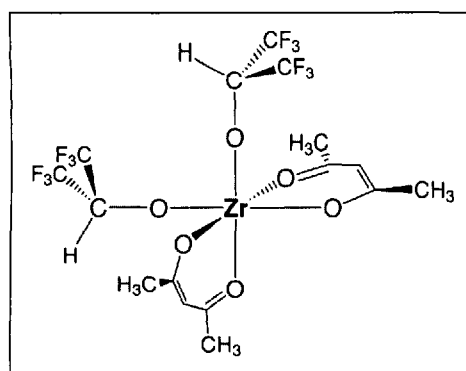

Fig. 5. *Molecular structure of zirconium precursor molecule Zr(acac)2[OCH(CF3)2]2* [10]

way are shown in *Fig. 3*. The potential for applications of such approaches in the biosensor area is clear.

While the thiol-gold SAM has been a boon to researchers, the need for a gold surface has limited its widespread biomedical applicability. Of potentially greater practical interest are systems that produce SAMs on oxide surfaces. Silanes have long been used [5] to surface-treat oxides, but it is only under exceptional conditions [6] that these are true SAMs, since the inherent cross-linking ability of silanes renders them susceptible to uncontrolled polymerization on the surface with the consequent formation of a multilayer. Very recently, it has been shown, however, that phosphates and phosphonates [7] can form true SAMs on flat oxides with similar packing and order to the corresponding gold-SAM systems. This is a new area with enormous promise for applications both in the biomedical as well as in the corrosion area.

While it is difficult to produce a true SAM using silanes, this is not always a critical issue. In the case of titanium, which, along with its alloys, finds considerable use as a dental and hip-implant material, we have been attempting to functionalize the surface with peptides using a silane-based approach. Certain peptide sequences are known to bind selectively to receptors on cells, and it is thought that the immobilization of such sequences on implants could stimulate their rapid integration into bone, *e.g.* Our approach [8] (*Fig. 4*) has been to immobilize a layer of an aminosilane on the OH-terminated oxide surface, following this with a cross-linker terminated on the one end with a succin-

amide and on the other with a maleimide functionality. The succinamide reacts with the free NH_2 group on the silane layer, leaving its maleimide end free to react with SH groups, with which it reacts under mild conditions. The main peptide investigated until now has been arginine-glycine-aspartic acid (RGD), which is present in fibronectin and known to interact selectively with certain cell receptors. This peptide is readily connected to another amino acid, cysteine, which contains the necessary SH group for reaction with the maleimide.

3. Tailored Surfaces with Potential Industrial Applications

Hard coatings of various kinds have found application in the machine tool industry for many years. A well-known example is the familiar gold-colored titanium-nitride coating, often found on drill bits. Such coatings are often applied by physical means. Physical vapor deposition (PVD) has the disadvantage, however, that the coatings are deposited in line-of-sight from the source, meaning that complex surface morphologies (as found on drill bits, *e.g.*) are difficult to coat evenly. Chemical vapor deposition (CVD), on the other hand, involves the chemical reaction of a gas-phase precursor with the substrate, with the consequence that even coatings can be produced on complex surfaces.

In our laboratory, we have been working on a successor material to TiN, namely zirconium nitride. This coating has been commercially produced on a limited scale using PVD, and our goal is to develop a CVD method for its production. ZrN has similar favorable wear resistance to TiN, but with the added advantage that it provides a surface with a much lower friction coefficient. This, in turn, leads to lower heat generation during machining operations, which translates to a reduction in the amount of cutting fluid necessary. This is very desirable, because disposal of used cutting fluid is a very costly enterprise, since it is often classified as hazardous waste, due to its high metal content.

Existing zirconium CVD precursors have been far from ideal: either they have required such high substrate temperatures for reaction that they could not be used for the coating of steel (due to the loss of substrate hardness), or they have displayed properties such as low volatility or extreme moisture sensitivity, which make their use in CVD difficult. We have developed a new generation of precursors, which

are both volatile and relatively moisture insensitive, and have used these to produce ZrN (and hard zirconia) coatings on a number of substrates [9]. *Figs. 5* and *6* show the molecular structure of the precursor [10], $Zr(acac)_2[OCH(CF_3)_2]_2$ and an electron micrograph of a zirconia-ceria bilayer, produced from the precursor.

Nanostructured surfaces have a number of applications as electrodes, in field-emission displays and in magnetic storage. An alternative to the frequently applied nanolithographic methods has been developed in our group. The approach (*Fig. 7*) is based upon the nanoscale porosity that is produced (in a controllable manner) in the oxide coating formed during the anodization of aluminum. Using electrochemical methods, this structure can be filled with a metal (such as nickel or gold), and the aluminum and oxide template wholly or partially etched away. The resulting 'forest' of nanotips is shown in *Fig. 8*.

4. Surface Analysis Methods

For many years, the classical approach to a problem by the surface scientist involved its reduction to a model involving single crystals. While this approach has had some success in some technologies (notably catalysis), in the case of highly complex systems such as biomaterials or
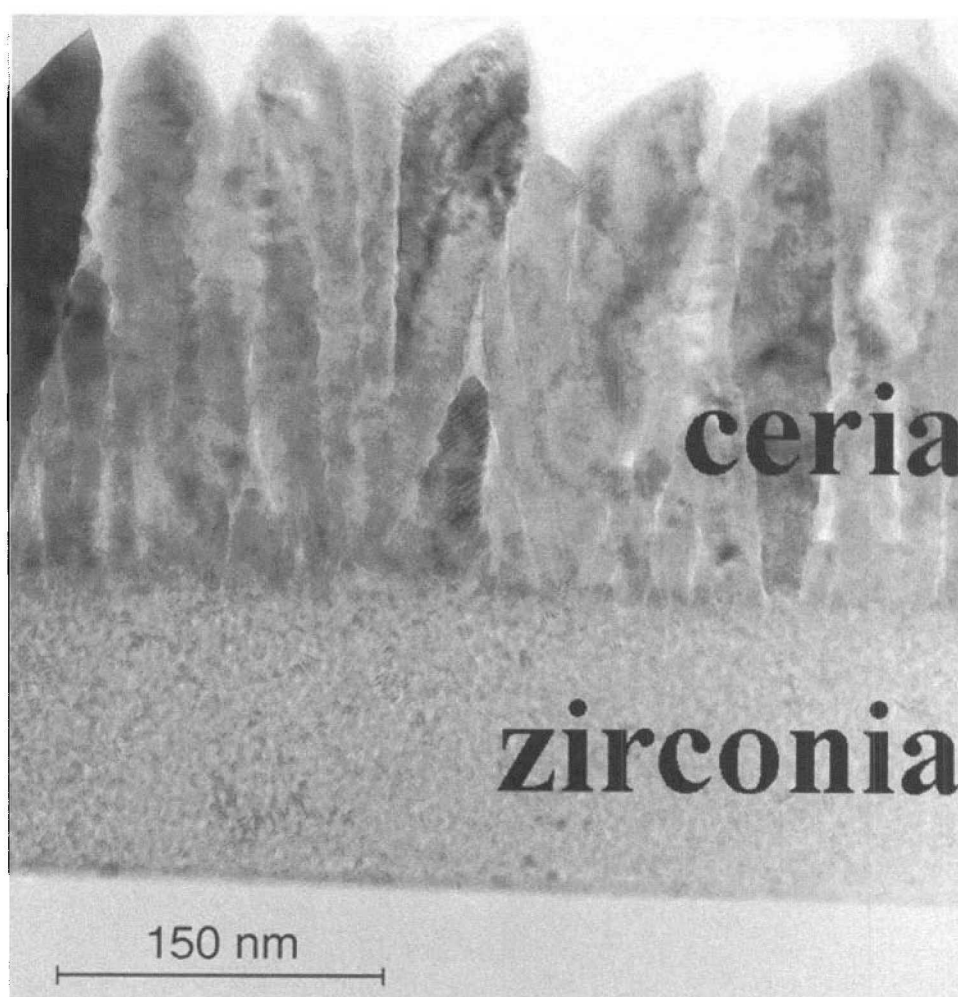
Fig. 6. *SEM photograph of a ceria-zirconia bilayer, prepared by CVD using* $Zr(acac)_2[OCH(CF_3)_2]_2$ *and a conventional ceria precursor,* $Ce(thd)_4$ [9]
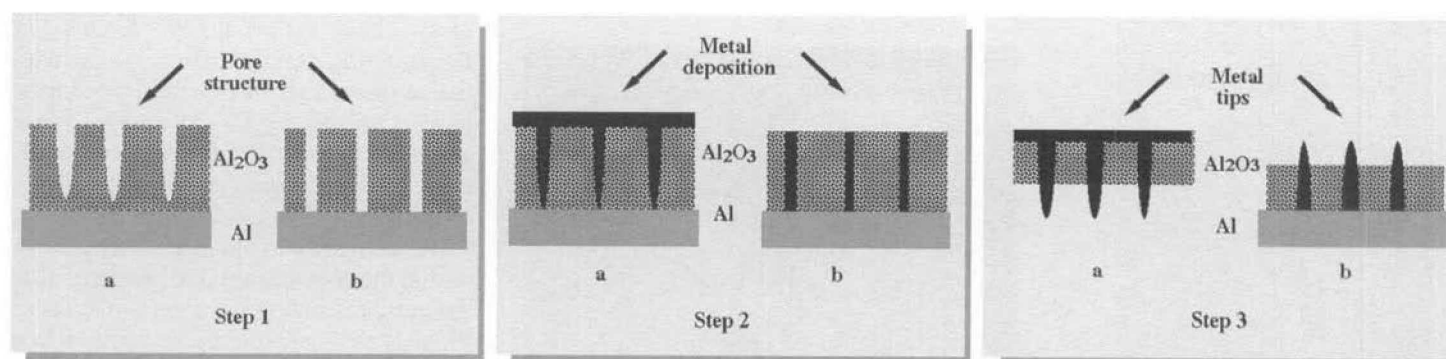
Fig. 7. *Fabrication of nanotip arrays by aluminum-oxide technology. Step 1*: Adjustable pore geometry and density by control of anodization conditions. *Step 2*: Electrolytic or chemical deposition of metals. *Step 3*: Selective removal of aluminum and oxide substrate [1].

tribosystems, this method is seldom useful. In the last decade or so, the advent of imaging incarnations of familiar ultrahigh-vacuum surface-analytical methods, such as *Auger* spectroscopy, X-ray photoelectron spectroscopy (XPS), and secondary-ion mass spectroscopy (SIMS), has opened up a new way of looking at spatially complex systems, and has often enabled properties to be more easily correlated with surface chemistry. We have focussed both on the application of such methods for the understanding of the surface chemistry of
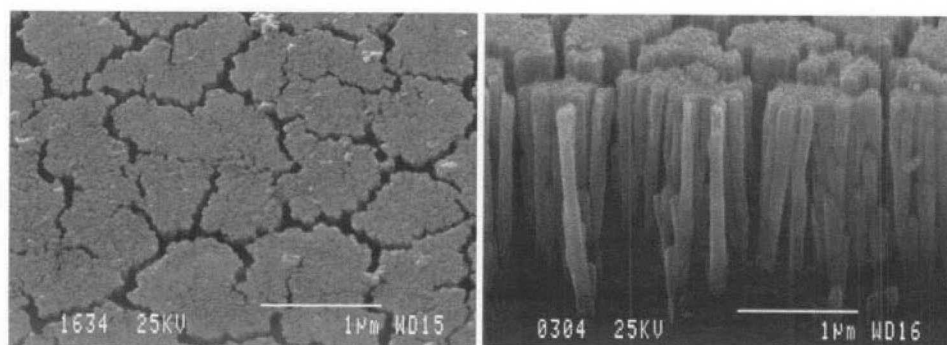
Fig. 8. *SEM photograph of a free-standing 'forest' of nickel nanotips (left*: top view, *right*: cross-sectional view) *prepared as shown in* Fig. 7 [11]
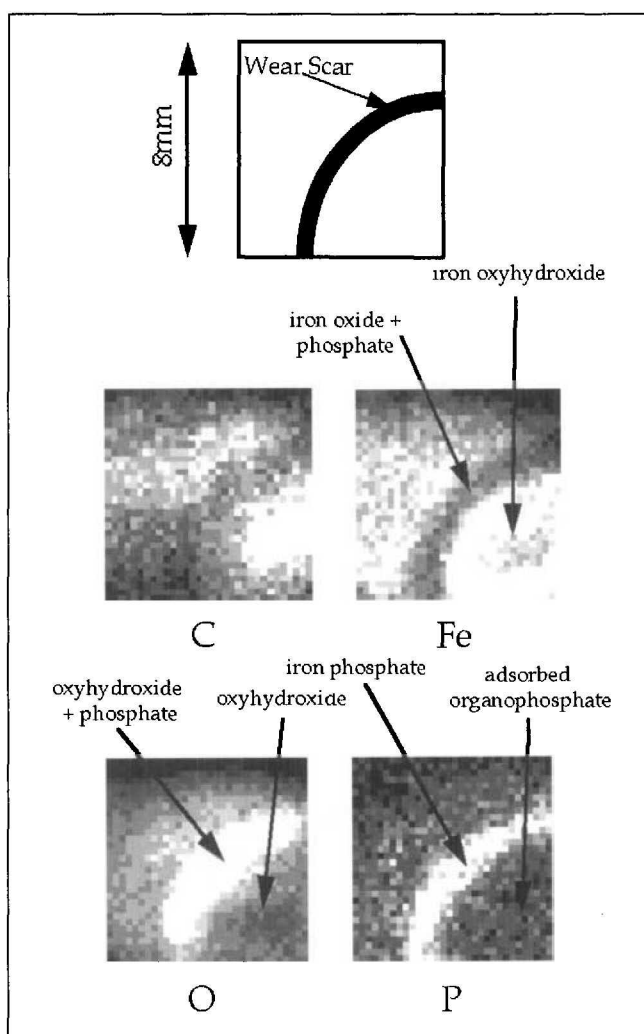
Fig. 9. *Imaging XPS analysis of steel surface following tribological testing of 100Cr6 steel in the presence of the phosphate-ester lubricant additive, Irgalube 349* (lighter areas correspond to higher intensity)

Fig. 10. Left: *Titanium for medical implants: artificial hip joint with TiAlNb stem.* Source: *Sulzer Orthopedics.* Right: *Dental implant with specially treated titanium surfaces for the parts in contact with the bone (rough) and gingiva (smooth).* Source: *Institut Straumann.*

advanced materials as well as on the development of new, spatially resolved surface-analytical methods.

One particularly industrially important surface interaction is that of lubricant additives with steel surfaces. Although many sliding surfaces in machinery are separated by oil films for most of the time, there are frequently situations (such as during startup, or under extreme contact pressure conditions, as is often found in gears) where the metal surfaces come virtually into contact. This situation can lead to unacceptable wear, unless appropriate additives are present in the lubricant. Many of these additives were discovered accidentally, and the mechanism by which they function is often unknown. Many of them are environmentally damaging, and, thus, a considerable effort is being put into their replacement with more benign alternatives. This is difficult, however, without understanding the way in which they work. We are using imaging X-ray photoelectron spectroscopy in order to improve this situation. *Fig. 9* shows several XPS images obtained after a steel disc was rubbed by a steel flat during a tribological test under a lubricant containing a phosphate ester/amine additive. From the images, it is possible to see that the additive has reacted with the steel substrate selectively within the contact area, forming an inorganic phosphate. Carbon, indicative of the unreacted organic phosphate, is chiefly to be seen in the surrounding, noncontact regions. Under the conditions employed in this test, nitrogen was not in evidence on the surface, suggesting that the amine played no tribological role under these conditions. Under more severe test conditions, similar results were obtained for oxygen, phosphorus, carbon, and iron, while nitrogen was also found selectively within the contact area. This suggests that the more extreme conditions had, indeed, induced a tribochemical reaction to switch on. Clearly, this approach has enormous potential for elucidating mechanisms of this kind.

Imaging techniques have also been valuable in determining the surface composition of titanium alloys employed as implant materials [12] (*Fig. 10*). Using the electron microprobe technique, which samples the top few microns of the material, it was demonstrated that the alloy Ti6Al7Nb consists of two phases, one rich in aluminum and one rich in niobium, compared to the overall composition (*Fig. 11*). Scanning *Auger* microscopy, which is far more surface-sensitive, showed that the native oxide layer reflects the composition of the underlying grains, and thus
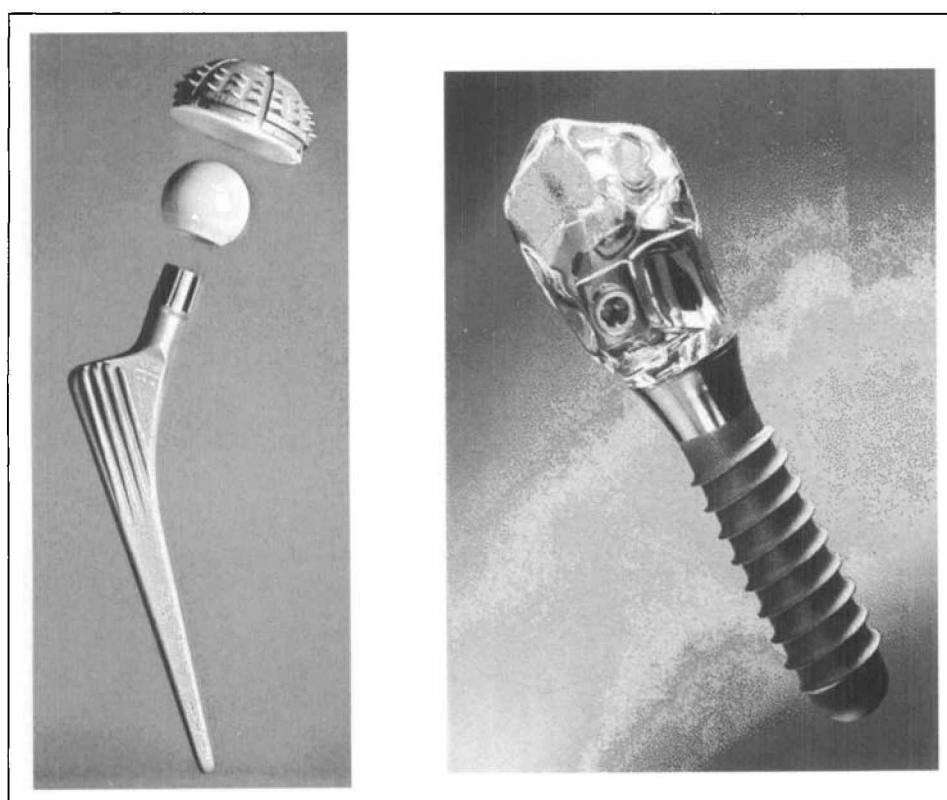
also displays Al-rich and Nb-rich phases (*Fig. 12*). This is significant, since different oxide compositions have different isoelectric points (IEPs), meaning that at the same pH of surrounding medium, they will have differing surface charges (possibly even of different sign). This can have a major effect on protein adsorption and, in turn, on cell adhesion and ultimate integration into the bone, for example.

The surface charge can be probed directly using atomic and lateral force microscopies (AFM and LFM). If an AFM experiment is carried out on an oxide sample under an electrolyte of a given pH, both tip (usually an oxynitride surface) and sample have characteristic charges, depending on their IEPs. These charges influence both the normal force between the tip and surface as well as the friction between them. Thus an LFM image (a frictional map of the surface) of the surface will change as a function of pH and the IEPs of the individual oxides. This is illustrated in *Fig. 13* for a model surface [13] and in *Fig. 14* for the Ti-Al-Nb alloy described above, where the difference in surface charge is represented by a difference in friction [14]. This technique is not only useful for examining surface charge, but can also be used as a spatially resolved surface-analytical technique for oxides, since the IEP is characteristic for a given oxide.

Other forces may also be capitalized upon, in order to characterize different materials surfaces. One example is the measurement of *van der Waals* forces between an AFM tip and polymer surfaces, in order to distinguish between different polymers. We have found [15] that by making AFM adhesion measurements between a silica-coated tip and a flat (spin-coated) polymer surface under the nonpolar, low-refractive-index liquid perfluorodecalin, we are able to differentiate between different polymers. Moreover, this behavior can be predicted by means of the *Lifshitz* equation [16][17], as follows:

$$A_{Total} = A_{v=0} + A_{v>0} \approx \frac{3}{4} kT \left(\frac{\varepsilon_1 - \varepsilon_3}{\varepsilon_1 + \varepsilon_3} \right) \left(\frac{\varepsilon_2 - \varepsilon_3}{\varepsilon_2 + \varepsilon_3} \right) +$$
$$\frac{3h\nu_e}{8\sqrt{2}} \frac{\left(n_1^2 - n_3^2 \right)\left(n_2^2 - n_3^2 \right)}{\left(n_1^2 + n_3^2 \right)^{1/2} \left(n_2^2 + n_3^2 \right)^{1/2} \left\{ \left(n_1^2 + n_3^2 \right)^{1/2} + \left(n_2^2 + n_3^2 \right)^{1/2} \right\}} ,$$
(1)

where the electronic absorption frequency ν_e is assumed to be equal for all three components ($\nu_e = 3 \cdot 10^{15}$ Hz). This equation relates the dielectric constants (ε_1, ε_2, ε_3) and refractive indices (n_1, n_2, n_3) of the two interacting surfaces and the intervening medium with the *Hamaker* constant A_{Total} and, therefore, the *van der Waals* interaction between the surfaces (*Fig. 15*).
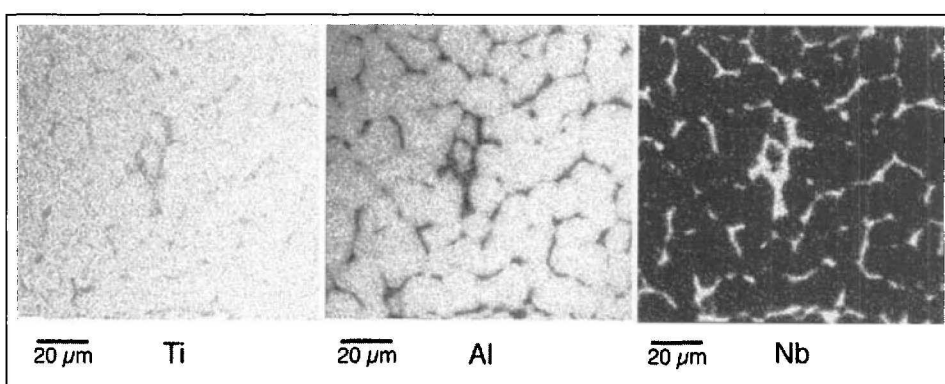

Fig. 11. *Electron microprobe map of a polished Ti6Al7Nb surface, showing distribution of the elements Ti, Al, and Nb* [13]
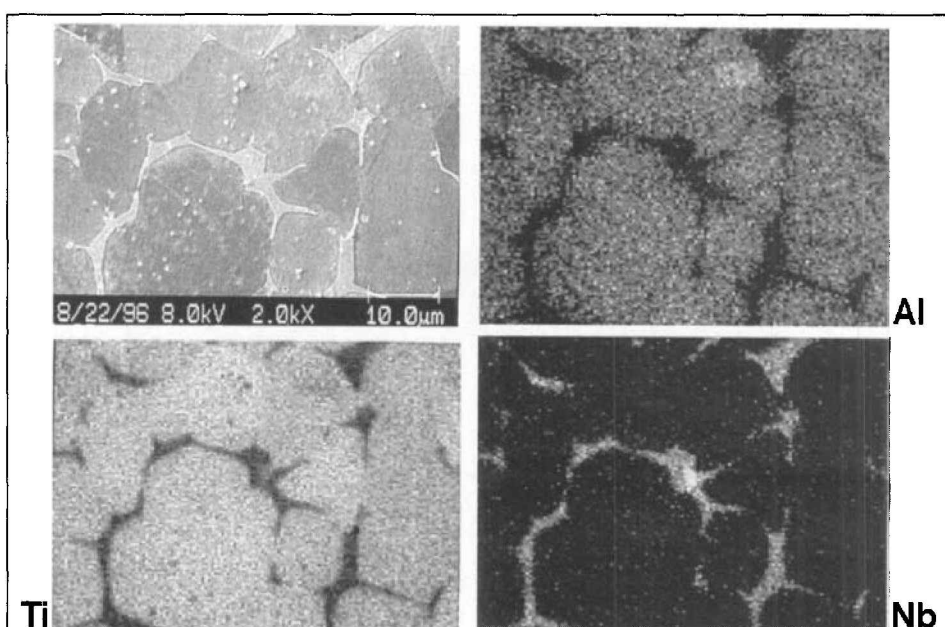

Fig. 12. *Scanning* Auger *micrograph (SAM) of a polished Ti6Al7Nb surface: electron image (topography) and distribution of the elements Ti, Al, and Nb* [14]

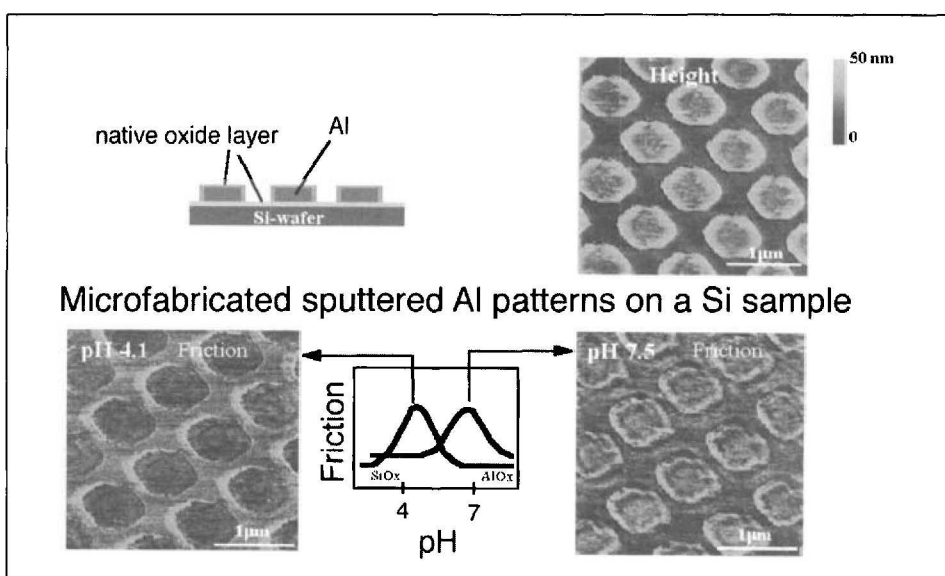Microfabricated sputtered Al patterns on a Si sample

Fig. 13. *The charge on oxidic surfaces (including that of the tip) changes as a function of pH-value when they are in contact with an electrolyte.* The pH-value at which the charge changes from + to – depends on the chemical nature of the oxide. The tip-sample charge interaction contributes to the friction measured or imaged (by LFM) for the system. A frictional image of a multicomponent oxide surface therefore changes as the pH of the electrolyte is varied, depending on the specific oxides involved [13].
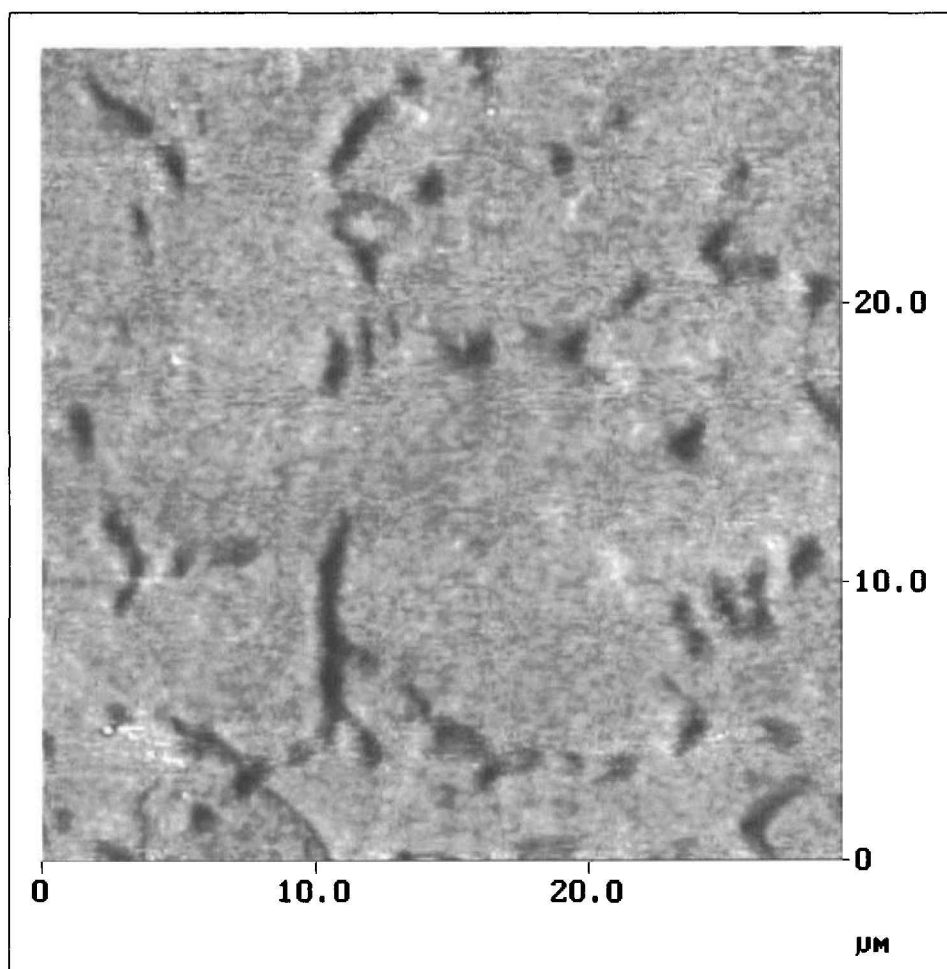
Fig. 14. *Lateral Force Microscopy image of a Ti-Al-Nb alloy surface under an electrolyte at pH 5.7, showing charge-induced frictional differences between oxide phases of different composition*

This difference in adhesion also leads to a contrast in friction, as measured by the Lateral Force Microscope, enabling PMMA and PS to be spatially distinguished, *e.g.*, with high resolution (*Fig. 16*).

Crucial in our studies of the titanium-biomolecule interaction has been the use of *in situ* methods for the monitoring of, *e.g.* protein adsorption [18]. One of the most fruitful approaches has been the use of the planar waveguide technique, optical waveguide lightmode spectroscopy (OWLS) [19]. The method is based on the incoupling of a laser into a waveguiding layer *via* a submicron grating (*Fig. 17*). The light is then guided by total internal reflection within the 150–200 nm thick waveguiding layer and its intensity detected at the lateral exits by photodiodes. The interaction of the evanescent wave with the liquid brought in contact with the waveguide surface leads to a change in the effective refractive index, from which the thickness of the layer can be calculated. The rate of change can also be readily followed, allowing kinetic measurements to be undertaken. The sensitivity of the method is approximately 1 ng cm^{-1}. The system will also function if a very thin layer of another material is deposited on top of the waveguide (*Fig. 18*), meaning that the interaction of molecules in an
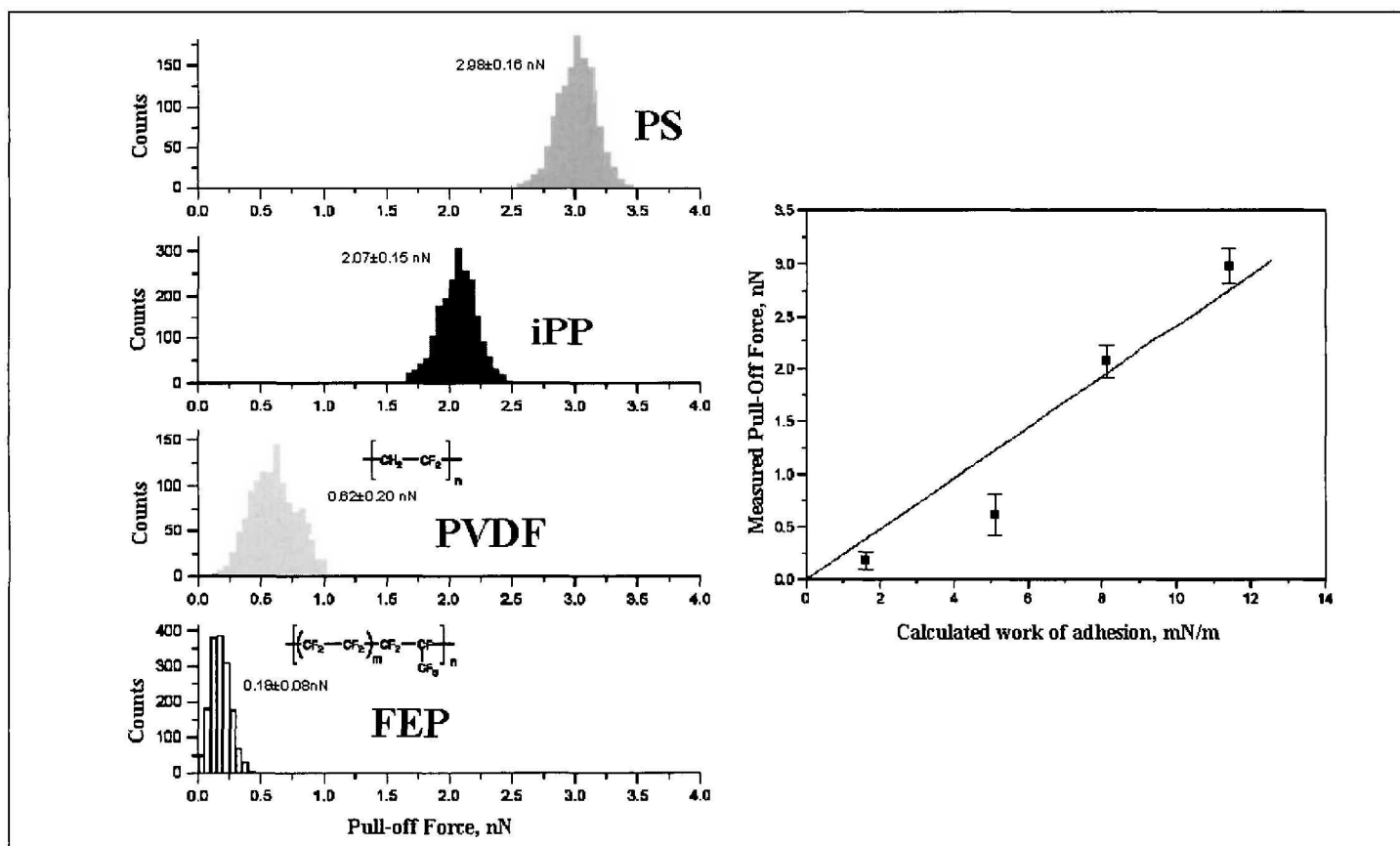

Fig. 15. *Histograms of measured pull-off forces (left) and comparison of measured pull-off forces and calculated work of adhesion (right) for a SiO$_x$ probe and PS, i-PP, PVDF, and FEP surfaces in perfluorodecalin* [15]

aqueous phase with virtually any coating can, in principle, be studied with this approach. In the course of our work on the TiAlNb hip-implant alloy, it was of interest to know how proteins adsorbed on the different oxides present on the metal surface. The results of our OWLS study are shown in *Fig. 19*, where the relative rates and total amounts of adsorption of fibronectin on TiO_2, Al_2O_3, and Nb_2O_5 can readily be seen. The oxides were coated as 5–20 nm layers onto the waveguide surface by means of magnetron sputtering. The method has also been used to examine the behavior of various coatings that have protein-resistance properties. *Fig. 20* shows the difference between serum protein adsorption on an uncoated (silica-titania) waveguide compared to a waveguide that had been pretreated with poly-lysine-polyethylene glycol [20]. The amount of serum adsorption is drastically reduced in the presence of the polymer.

5. Conclusion

The use of tailored, advanced surfaces, in order to impart useful properties to bulk substrates is now widespread in many fields of industry and medicine. Nevertheless, there is still tremendous scope for the development of new surface treatments and functionalization methods. This is particularly true in the case of biocompatible and bioactive coatings, where the interaction of surfaces with the biological environment is only just beginning to be understood.

With the development of new surfaces comes the need for methods that enable us to analyze these surfaces and monitor their interactions with the environment. Imaging techniques can play an important role here, as well as methods that enable *in situ* examination of the surfaces under the conditions in which they might ultimately be applied.
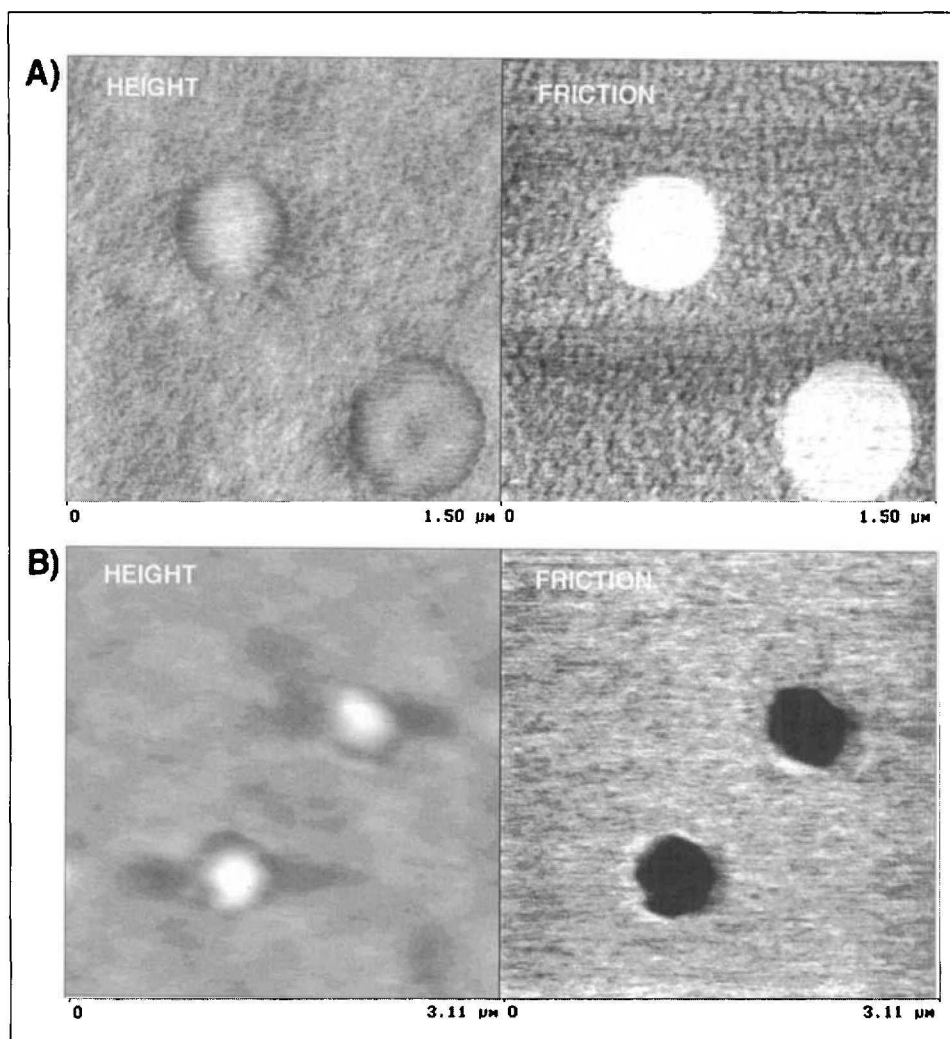
Fig. 16. *Height (AFM) and friction (LFM) images of a spin-cast polystyrene: poly(methyl methacrylate) polymer blend [PS:PMMA (1:10 w:w)], obtained with* a) *gold-coated and* b) *SiO$_2$ tips under perfluorodecalin* [15]
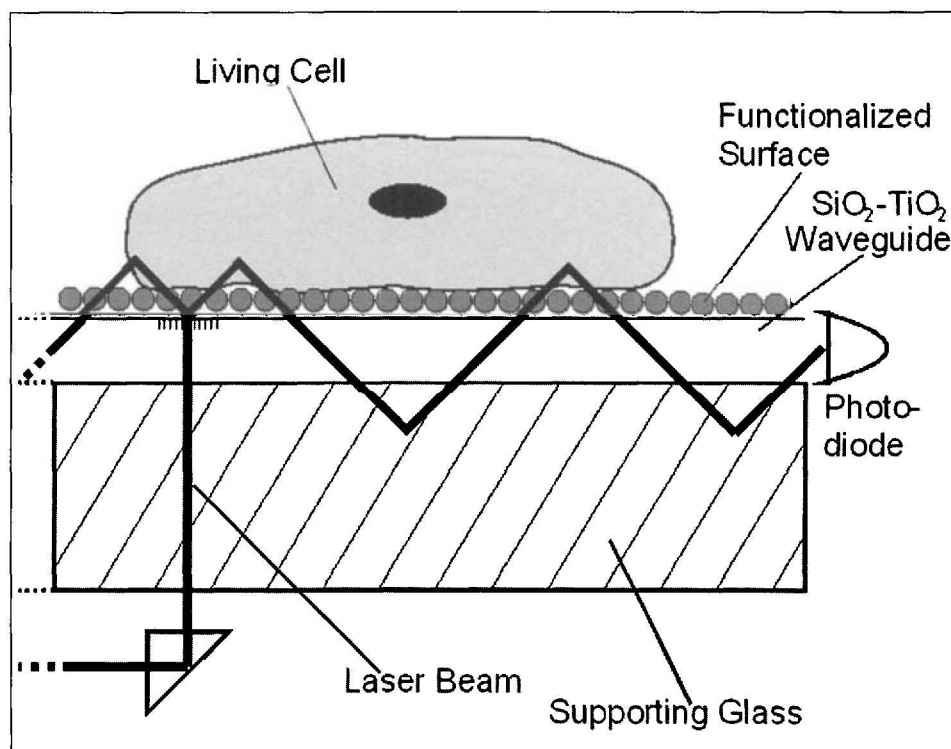

Fig. 17. *Schematic drawing of the planar waveguide technique for* in situ *studies of biomolecule and cell interactions with transparent surfaces* [18]
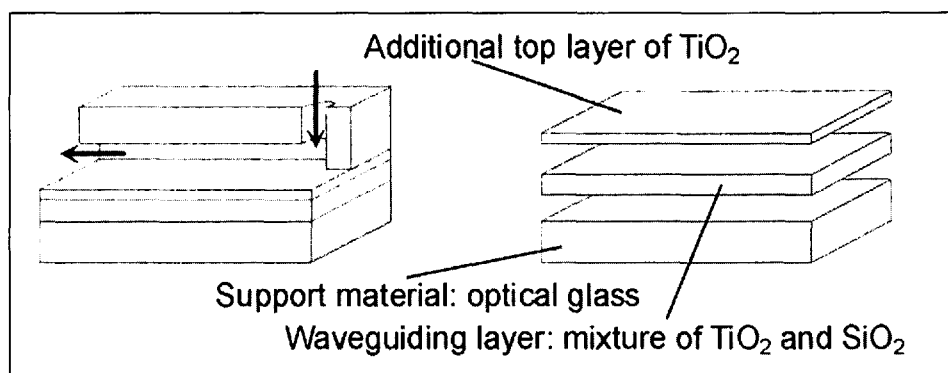
Fig. 18. *Planar waveguide with additional top coating to study the effect of surface composition on adsorption of biomolecules* [18]
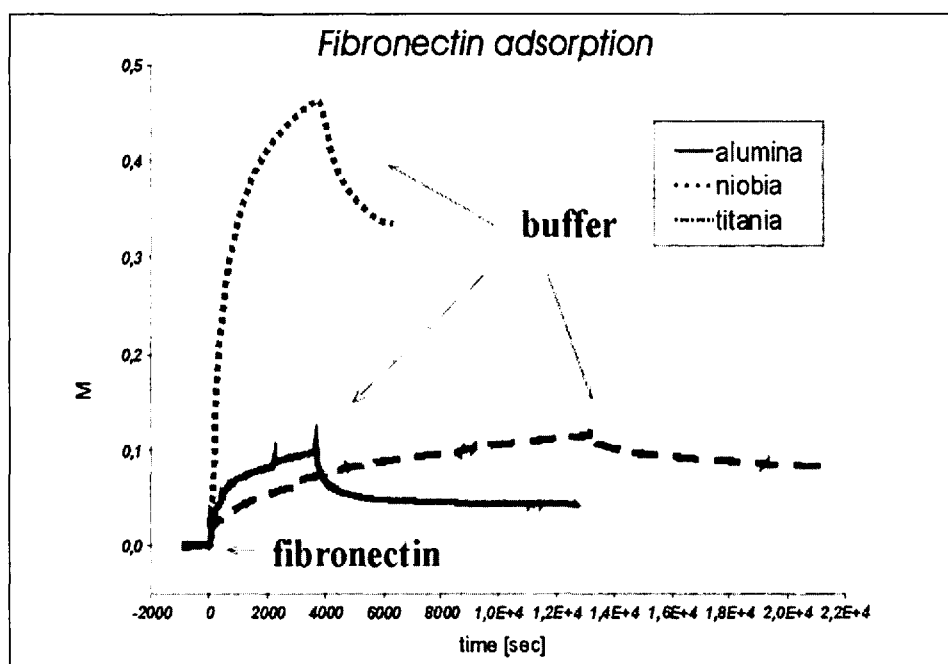

Fig. 19. *Adsorption curves (mass in µg/cm²) for the protein fibronection on waveguide surfaces with top layers of titania, alumina, and niobia.* Protein adsorption followed by rinsing in PBS buffer [18].
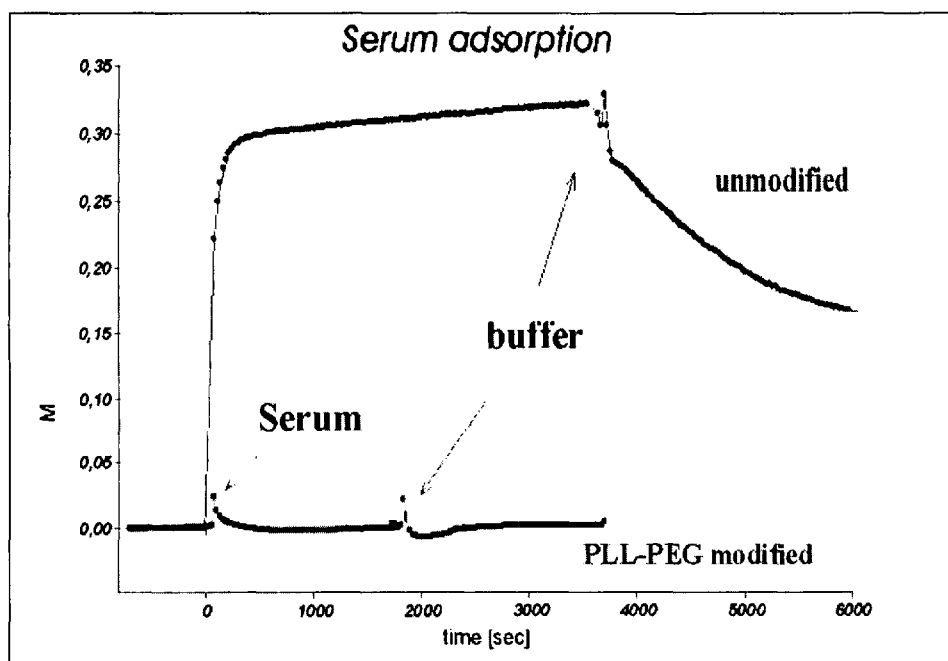

Fig. 20. *Comparative serum adsorption curves (adsorbed mass M in µg/cm²) as a function of time for a silica-titania waveguide surface with and without a preadsorbed layer of polylysine-polyethylene glycol (PLL-PEG), studied using optical waveguide techniques.* The amount of adsorbed serum proteins is drastically reduced in the case of the PLL-PEG-modified surface [18].

[1] C.D. Bain, E.B. Troughton, Y.-T. Tao, J. Evall, G.M. Whitesides, *J. Am. Chem. Soc.* **1989**, *111*, 321; R.G. Nuzzo, D.L. Allara, *ibid.* **1983**, *105*, 4481; M.D. Porter, T.B. Bright, D.L. Allara, C.E.D. Chidsey, *ibid.* **1987**, *109*, 3559; H. Sellers, A. Ulman, Y. Schnidman, J.E. Eilers, *ibid.* **1993**, *115*, 9389; A.R. Bishop, R.G. Nuzzo, *Curr. Opin. Coll. Interf. Sci.* **1996**, *1*, 127; A. Ulman, *Chem. Rev.* **1996**, *96*, 1533.
[2] M.C. Fritz, G. Hähner, N.D Spencer, R. Bürli, A. Vasella, *Langmuir* **1996**, *12*, 6074.
[3] F.G. Zaugg, P. Wagner, P. Kernen, A. Vinckier, P. Groscurth, N.D. Spencer, G. Semenza, *J. Mat. Sci.: Mat. Med.*, in press.
[4] J.L. Wilbur, E. Kumar, G.M. Whitesides, *Adv. Mater.* **1994**, *6*, 600; M. Mrksich, G.M. Whitesides, *Trends Biotechnol.* **1995**, *13*, 228; Y. Xia, G.M. Whitesides, *Angew. Chem. Int. Ed. Engl.* **1998**, *37*, 550.
[5] A. Ulman, 'Ultrathin Organic Films', Academic Press, San Diego, CA, 1991.
[6] N.L. Jeon, K. Finnie, K. Branshaw, R.G. Nuzzo, *Langmuir* **1997**, *13*, 3382.
[7] J.T. Woodward, A. Ulman, D.K. Schwartz, *Langmuir* **1996**, *12*, 3626.
[8] S.J. Xiao, M. Wieland, B. Keller, H. Siegrist, M. Textor, N.D. Spencer, *J. Mat. Sci.: Mat. Med.* **1997**, *8*, 867.
[9] M. Morstein, I. Pozsgai, N.D. Spencer, 'Chemical Vapor Deposition, Proceedings of CVD. XIV and EUROCVD-11', Electrochemical Society Proceedings Series 1997, Vol. 97–25, p. 976.
[10] M. Morstein, *Inorg. Chem.*, submitted.
[11] F. Schlottig, M. Textor, N.D. Spencer, K. Sekinger, U. Schnaut, J.-F. Paule, *Fresenius J. Anal. Chem.*, submitted.
[12] C. Sittig, M. Wieland, P.-H. Vallotton, M. Textor, N.D. Spencer, *J. Mat. Sci.: Mat. Med.*, in press.
[13] G. Hähner, A. Marti, N.D. Spencer, *Tribology Lett.* **1997**, *3*, 359.
[14] C. Sittig, G. Hähner, A. Marti, R. Hauert, M. Textor, N.D. Spencer, *J. Mat. Sci.: Mat. Med.*, in press.
[15] K. Feldman, T. Tervoort, P. Smith, N.D. Spencer, *Langmuir* **1998**, *14*, 372.
[16] J.Israelachvili, 'Intermolecular and Surface Forces', 2nd edn., Academic Press, London, 1992, Chapt. 11.
[17] E.M. Lifshitz, *Sov. Phys.* **1956**, *JETP* 2, 73.
[18] N.D. Spencer, M. Textor, 'Materials in Medicine', Eds. M.O. Speidel, P. Uggowitzer, vdf, Zürich, 1998, p. 209.
[19] R. Kurrat, J.J. Ramsden, J.E. Prenosil, *J. Chem. Soc., Faraday Trans.* **1994**, *90*, 587.
[20] D.L. Elbert, J.A. Hubbell, *Chem. Biol.* **1998**, *5*, 177.